CHAPTER – 4

APPLICATION OF THE PROPOSED EXCITATION CONTROL STRATEGY IN MULTIMACHINE POWER SYSTEM

4.1 Introduction:

Power systems are large-scale systems spread over wide geographical areas. Such widely distributed structure of power systems makes it difficult to implement any centralized control facility for transient stability enhancement. Although overwhelming advancement has been done in the area of data communication and remote measurement, centralized scheme for transient stability enhancement of a large multimachine power system is not yet achievable. This is due not only to the amount of data to be collected at the central location, but also to the amount of computations to be carried out which is quite large with respect to the time frame of transient stability control. This makes decentralized control the most suitable option for transient stability enhancement of multimachine power systems.

Research results on decentralized nonlinear excitation control for multimachine power system transient stability improvement have been reported [44, 45] in various publications. Most of these methods [44, 45] are extensions of the result of ref. [42] to the multimachine case. The DFL excitation control technique has been extended to multimachine power systems to eliminate the nonlinearities and interconnections. The DFL compensated generator model in this case still contains nonlinearities due to interconnections with other generators in addition to the parametric uncertainty in the linearized model of the generator. The robust control technique [42] is then extended to the interconnected uncertain DFL compensated model to design the robust feedback controller. In this control scheme, only the bounds of the generator parameters need to be known but not the network parameters, system operating points or fault locations. This simplifies the problem of determination of the uncertainty bounds by a great deal, but the overall problem solution is still much involved computationally. Moreover, how the bounds on the generator parameters can be determined is not clear.

In the previous chapter it has been shown that the proposed DFL control strategy can exhibit complete robustness to external system disturbances such as unpredictable changes in transmission line reactances (and also changes in the infinite bus voltage) in an SMIB power system. Hence, in a multi machine system it takes into account all the effects of interconnections and renders the DFL compensated generator completely immune to all nonlinearities and uncertainties arising from the external system

Moreover, the DFL control law can be implemented at the generator terminals. So, the proposed control law is a decentralized control law, and, can be applied for robust decentralized excitation control in a multimachine power system without any additional consideration or modifications. The proposed DFL compensator makes the linearized generator model completely decoupled from the interaction terms with other remote generators. The effect of interactions, which has been taken into account by previous authors [45] as parametric uncertainties, is incorporated automatically within the proposed control law (see Appendix) in terms of locally measurable or computible quantities. In this chapter, the effectiveness of the proposed control strategy has been demonstrated by simulation results of a 3-machine power system [45]. Comparison of performance of the proposed controller with that of the previous controller [45] is shown in the simulation results.

4.2 Existing Decentralized Controller:

In the design of the existing robust nonlinear decentralized excitation controller [45] the DFL control technique [42] for SMIB power system has been extended to multimachine power systems. The procedure is discussed briefly below:

Power System Model:

Using suffix ‘i’ for the ith machine quantities and suffix ‘j’ for the jth one the dynamical model of the ith (i = 1,2,…….n) machine in an n-machine power system can be written as [45].

$$\dot{\delta}_i(t) = \omega_i(t) - \omega_o \qquad (4.1)$$

$$\dot{\omega}_i(t) = -\frac{D_i}{2H_i}\omega_i(t) + \frac{\omega_o}{2H_i}\left[P_{m_i} - P_{e_i}(t)\right] \quad (4.2)$$

$$\dot{E}'_{q_i}(t) = \frac{1}{T'_{do_i}}\left[E_{f_i}(t) - E_{q_i}(t)\right] \quad (4.3)$$

$$E_{q_i}(t) = E'_{q_i}(t) + (x_{di} - x'_{di})I_{d_i}(t) \quad (4.4)$$

$$P_{e_i}(t) = \sum_{j=1}^{n} E'_{q_i}(t)E'_{q_j}(t)Y'_{ij}\sin\left(\delta_{ij}(t)\right) \quad (4.5)$$

$$Q_{e_i}(t) = -\sum_{j=1}^{n} E'_{q_i}(t)E'_{qj}Y'_{ij}\cos\left(\delta_{ij}(t)\right) \quad (4.6)$$

$$I_{d_i}(t) = \sum_{j=1}^{n} E'_{qj}(t)Y'_{ij}\cos\left(\delta_{ij}(t)\right) = -\frac{Q_{ei}(t)}{E'_{qi}(t)} \quad (4.7)$$

$$I_{q_i}(t) = \sum_{j=1}^{n} E'_{qj}(t)Y'_{ij}\sin\left(\delta_{ij}(t)\right) = \frac{P_{ei}(t)}{E'_{qi}(t)} \quad (4.8)$$

$$E_{fi}(t) = k_{e_i}u_{f_i}(t) \quad (4.9)$$

$$E_{qi}(t) = x_{ad_i}I_{f_i}(t) \quad (4.10)$$

Where,

$\delta_{ij}(t) = \delta_i(t) - \delta_j(t)$

Y'_{ij} is the transfer admittance between internal nodes of ith and jth generators.

All other terms have been defined in section 3.2 of chapter 3 and have been used here with appropriate suffixes.

It may be noted that in the above power system model, the network is reduced to generator internal nodes, and, the generators are modeled as the voltage behind direct axis transient reactances with flux decay dynamics.

The DFL Compensator:

Differentiating equation (4.5) and using equations (4.1) – (4.9) the following DFL compensated power system model is obtained [45]:

$$\Delta\dot{\delta}_i(t) = \Delta\omega_i(t) \tag{4.11}$$

$$\Delta\dot{\omega}_i(t) = -\frac{D_i}{2H_i}\omega_i(t) - \frac{\omega_o}{2H_i}\Delta P_{ei}(t) \tag{4.12}$$

$$\Delta\dot{P}_{ei}(t) = -\frac{1}{T'_{do_i}}\Delta P_{ei}(t) + \frac{1}{T'_{do_i}}v_{fi}(t) + \sum_{j=1}^{n} E'_{qi}(t)\dot{E}'_{qi}(t)Y'_{ij}\sin\left(\delta_{ij}(t)\right) - E'_{qi}(t)\sum_{j=1}^{n} E'_{qi}(t)Y'_{ij}\cos\left(\delta_{ij}(t)\right)\omega_j(t) \tag{4.13}$$

Where,

$\Delta\delta_i(t) = \delta_i(t) - \delta_{oi}$; ($\delta_{\text{oi}}$ is the desired equilibrium value of $\delta_{\text{i}}(t)$

$\Delta\omega_i(t) = \omega_i(t) - \omega_o$

$\Delta P_{ei}(t) = P_{ei}(t) - P_{mi}$ and

$$v_{fi}(t) = k_{ei}u_{fi}(t)I_{qi}(t) + (x_{di} - x'_{di})I_{di}(t)I_{qi}(t) - T'_{do_i}Q_{ei}(t)\omega_i(t) - P_{mi} \tag{4.14}$$

The resulting DFL compensating law for the ith machine is given by

$$u_{fi}(t) = \frac{1}{k_{ei}I_{qi}(t)}\left[v_{fi}(t) - (x_{di} - x'_{di})I_{di}(t)I_{qi}(t) + T'_{do_i}Q_{ei}(t)\omega_i(t) + P_{mi}\right] \tag{4.15}$$

It can be noted that the mapping equation (4.15) froim $u_{fi}(t)$ to $v_{fi}(t)$ is invertible except for $I_{qi}(t) = 0$, which is not in the normal working region. The DFL law is practically realizable using only local measurements.

In equation (4.13), the terms $E'_{qi}(t)$, $\delta_j(t)$ and $\Delta\omega_I(t)$ represent the effects of remote dynamics of the jth generator on the ith one. the DFL controller does not cancel these remote dynamics. As a result, the DFL compensated model (equation (4.11) – (4.13)) contains the nonlinearities and interconnections. So, a robust control technique is employed for the DFL compensated model to ensure the stability of the multimachine power system irrespective of operating points and network parameter changes. In the robust controller designed by the authors [45] the uncertainties related to the network transmission parameters and interconnections have been treated as model parametric uncertainties and the robust stabilizing control is obtained by solving the resulting algebraic Riccati equation [45]. Their approach involves complex mathematics, and, moreover, their control strategy is difficult to realize practically mainly because the bounds of the parametric uncertainties are not easy to determine in a practical power system.

4.3 Prospect of the Proposed DFL Excitation Controller as Robust Decentralized Controller in Multimachine Power System:

For the ith generator model (equation (4.1) – (4.10)) an alternative DFL control law can be derived in the following way:

Using equation (4.8) and differentiating it

$$\dot{P}_{e_i}(t) = \dot{E}'_{q_i}(t)I_{q_i}(t) + E'_{q_i}(t)\dot{I}_{q_i}(t)$$

$$= \frac{1}{T'_{do_i}}\left[E_{f_i}(t) - E_{q_i}(t)\right]I_{q_i}(t) + E'_{q_i}(t)\dot{I}_{q_i}(t)$$

$$= \frac{1}{T'_{do_i}}k_{e_i}u_{f_i}(t)I_{q_i}(t) - \frac{1}{T'_{do_i}}\left[E'_{q_i}(t) + \left(x_{d_i} - x'_{d_i}\right)I_{d_i}(t)\right]I_{q_i}(t) + E'_{q_i}(t)\dot{I}_{q_i}(t)$$

$$= \frac{1}{T'_{do_i}} k_{e_i} u_{f_i}(t) i_{qi}(t) - \frac{1}{T'_{do_i}} P_{e_i}(t) - \frac{1}{T'_{do_i}} \left[\left(x_{d_i} - x'_{d_i} \right) i_{d_i}(t) \right] i_{q_i}(t) + E'_{q_i}(t) i_{q_i}(t)$$

$$= -\frac{1}{T'_{do_i}} P_{e_i}(t) + \frac{1}{T'_{do_i}} \left[k_{e_i} u_{f_i}(t) i_{q_i}(t) - \left(x_{d_i} - x'_{d_i} \right) i_{d_i}(t) i_{q_i}(t) + T'_{do_i} E'_{q_i}(t) i_{q_i}(t) \right]$$

$$\therefore \Delta \dot{P}_{e_i}(t) = \frac{1}{T'_{do_i}} \Delta P_{e_i}(t) + \frac{1}{T'_{do_i}} v_{f_i}(t) \tag{4.16}$$

where,

$$v_{f_i}(t) = k_{e_i} u_{f_i}(t) i_{q_i}(t) - \left(x_{d_i} - x'_{d_i} \right) i_{d_i}(t) i_{q_i}(t) + T'_{do_i} E'_{q_i}(t) i_{q_i}(t) - P_{m_i} \tag{4.17}$$

and the alternative DFL compensating law is given by

$$u_{f_i}(t) = \frac{1}{k_{e_i} i_{q_i}(t)} \left[v_{f_i}(t) + \left(x_{d_i} - x'_{d_i} \right) i_{d_i}(t) i_{q_i}(t) - T'_{do_i} E'_{q_i}(t) i_{q_i}(t) + P_{m_i} \right] \tag{4.18}$$

The alternative DFL control law (equation (4.18) is practically realizable by the use of locally measurable quantities, and it yields a completely decoupled linearized model for the ith machine as no interconnection terms appear in equation (4.16).

However, it may be noted that the single-axis generator model (equations (4.1) – (4.10)) with flux decay dynamics is a comparatively crude model for transient stability simulation studies. The DFL compensating law (equation (3.21)) proposed in chapter – 3 is derived from the two-axis model (equations (3.1) – (3.9)) of the generators which represents machine dynamics more accurately in transient stability simulation studies, and, therefore, is a better model for control development and studies of control effects. It has been shown in appendix – II that all the nonlinearities and interconnection terms appearing when the existing DFL technique [45] is applied to the ith machine represented by two-axis model (instead of the single-axis model) in a multimachine power system is incorporated within the newly proposed DFL control law.

Using suffix *i* for the ith machine quantities, the proposed DFL control law for the ith machine can be written as

$$u_{f_i}(t) = \frac{1}{k_{e_i} I_{q_i}(t)} \left[\hat{v}_{f_i}(t) - T'_{do_i} \left\{ E_{q_i}(t) i_{q_i}(t) + \left(x_{d_i} - x'_{d_i} \right) i_{d_i}(t) I_{q_i}(t) \right\} + P_{m_i} \right]$$

where,

$$\hat{v}_{f_i}(t) = k_{e_i} u_{f_i}(t) I_{q_i}(t) + T'_{do_i} \left[E_{q_i}(t) i_{q_i}(t) + \left(x_{d_i} - x'_{d_i} \right) i_{d_i}(t) I_{q_i}(t) \right] - P_{m_i}$$

$u_{fi}(t)$ is practically realizable only with the help of quantities measurable or available locally. Further, it extracts a linear model for the ith machine which is completely decoupled from the interactions with the dynamics of the remote machines. $\ddot{U}_{fi}(t)$ can be determined by any suitable method of control theory. In the present work, LQ optimal control method has been employed to determine $\ddot{U}_{fi}(t)$ which delivers a linear state feedback law of the following form:

$$\hat{v}_{fi}(t) = -\hat{K}_{\delta i} \Delta\delta_i(t) - \hat{K}_{\omega i} \Delta\omega_i(t) - \hat{K}_{pi} \Delta P_{ei}(t)$$

To obtain the states $\Delta\delta_I(t)$, $\Delta\omega_I(t)$ and $\Delta P_{ei}(t)$, the desired equilibrium values of $\delta_I(t)$, $\omega_I(t)$ and $P_{ei}(t)$, are necessary. While the equilibrium values for $\omega_I(t)$ and $P_{ei}(t)$ are readily known, that for $\delta_I(t)$ are available only after a full scale load flow calculation. This difficulty can be alleviated by applying the observation decoupled state space [62] which is very useful during the regime of emergency control in a power system. However, for simplicity, in the present work post-fault equilibrium values of $\delta_I(t)$ have been taken as known quantities (determined by load flow solution of the post fault network).

In the following sections, the effectiveness of the proposed DFL controller as decentralized excitation controller for transient stability improvement of multimachine power system has been illustrated by simulation results.

4.4 The Study System:

The three-machine power system shown in Fig.4.1 has been selected to illustrate the effectiveness of the proposed excitation controller in transient stability improvement of multimachine power system. The system data used in the simulation are available in ref. [13, 45] and also produced here for ready reference.

The system parameters are as follows:

x_{d1} = 1.863 p.u., x'_{d1} = 0.257 p.u., x_{T1} = 0.129 p.u., T'_{do1}= 6.9 secs.
H_1 = 4 secs, D_1 = 5 p.u., k_{e1} = 1.

x_{d2} = 2.36 p.u., x'_{d2} = 0.319 p.u. , x_{T2} = 0.11 p.u., T'_{do2} = 7.96 secs,
H_2 = 5.1 secs., D_2 = 3 p.u., k_{e2} = 1.

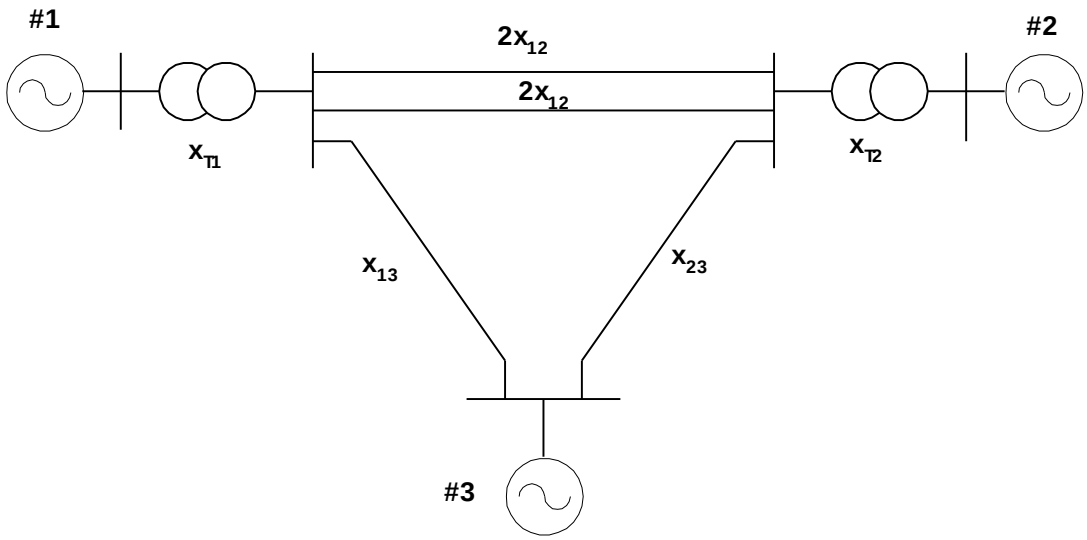

Fig.4.1 Three-machine example system

x_{12} = 0.55 p.u. , x_{13} = 0.53 p.u. , x_{23} = 0.6 p.u.

$x_{ad1} = x_{ad2} = 1.712$ p.u., $\omega_o = 314.159$ rad/sec.

$$-3 \le E_{fi}(t) = k_{ei}\, u_{fi}(t) \le 6 \;\; ; \;\; i = 1, 2$$

Generator #3 is an infinite bus with its terminal voltage (= internal voltage) constant at $1\angle 0^o$ p.u.

Following pre-fault operating points have been considered in the simulation:

Case – I: $\delta_{10} = 64.17^o$, $P_{m10} = 1.1$ p.u. , $V_{t1} = 1.0$ p.u.

$\delta_{20} = 63.025^o$, $P_{m20} = 1.0$ p.u. , $V_{t2} = 1.0$ p.u.

Case – II: $\delta_{10} = 48.51^o$, $P_{m10} = 0.3$ p.u. , $V_{t1} = 0.95$ p.u.

$\delta_{20} = 63.68^o$, $P_{m20} = 0.4$ p.u. , $V_{t2} = 0.95$ p.u.

The fault considered in the simulation is a symmetrical 3-phase short circuit fault that occurs on one of the transmission lines between generator #1 and generator #2. λ is the fraction of the line length to the left of the fault point. If $\lambda = 0$, the fault is on the h.t. bus of transformer T_1, $\lambda = 0.5$ means fault at the midpoint of the line and so on. The following fault sequences have been considered:

Sequence I : **(Temporary fault)**

Stage 1: The system is in pre-fault steady – state.

Stage 2: A fault occurs at t_o .

Stage 3: The fault is removed by opening the breakers of the faulted line at t_1

Stage 4: The transmission lines are restored with the fault cleared at t_2 .

Stage 5: The system is in post fault state.

Sequence II : **(Permanent fault)**

Stage 1: The system is in pre-fault steady – state.

Stage 2: A fault occurs at t_o .

Stage 3: The fault is removed by opening the breakers of the faulted line at t_1

Stage 4: The system is in post fault state.

The gain co-efficients determined by LQ optimal control technique for the two generators are as follows:

$$\hat{K}_{\delta 1} = -22.3607; \quad \hat{K}_{\omega 1} = -7.8317; \quad \hat{K}_{p1} = 55.4999$$
$$\hat{K}_{\delta 2} = -18.1532; \quad \hat{K}_{\omega 2} = -8.2106; \quad \hat{K}_{p2} = 63.4830$$

Different pre-fault operating points, different fault sequences and different fault locations have been considered to test the robustness of the control strategy. The following section illustrates the simulation results.

4.5 Simulation Results:

This section shows the simulation results to illustrate the effectiveness of the proposed DFL excitation controller in multimachine power system. Fig.4.2(a) to 4.2(l) demonstrates the results for operating point II. For all cases the fault inception time, t_o = 0.1 secs. Fig.4.2(a) and 4.2(b) shows that when the fault is very close to the H.T. terminals of transformer x_{T1}(λ=0.005) generator # 1 becomes unstable for a fault clearing time, t_1 = 0.66 secs. and remains stable at a fault clearing time, t_1 = 0.64 secs. But the post-fault response is highly oscillatory. Fig. 4.2(c) shows that with the proposed control, generator # 1 remains stable for t_1 = 0.66 secs. and good post-fault response is also achieved. Fig.4.2(d) to 4.2(g) shows the cases for different fault locations and fault clearing times. For all instances the proposed controller improves the 1st swing and produces good post-fault response with fairly rapid convergence to the post-fault equilibrium. Fig.4.2(h) to 4.2(j) shows the results when the fault is very close to the H.T. terminals of transformer x_{T2} (λ=0.99). From Fig.4.2(h) and 4.2(i) it is clear that generator # 2 becomes unstable for a fault clearing time, t_1 = 0.52 secs. and remains stable for t_1 = 0.5 secs., however, the post-fault response is undesirable. The effectiveness of the proposed controller is demonstrated in Fig.4.2(j) which shows appreciable reduction in the 1st swing as well as the post-fault oscillations. Fig.4.2(k) and 4.2(l) demonstrate the result when reclosing takes place at t_2 = 1.2 secs. From these two figures it is clear that the proposed controller is insensitive to such network changes. Fig.4.3(a) to 4.3(f)

demonstrate the simulation results for operating point – I for different fault locations and fault clearing times. While Fig.4.3(a), 4.3(c) and 4.3(e) illustrate the performance of the proposed control strategy for fault sequence – II, Fig. 4.3(b), 4.3(d) and 4.3(f) display the same for fault sequence – I for the reclosing time, t_2 = 1.2 secs. In all the above cases it can be seen that the controller performance is highly satisfactory. From all these results obtained for various conditions it can be concluded that the proposed excitation controller gives highly robust performance with respect fault locations, fault clearing times and network configurations.

Fig.4.2(a): power angle response without excitation control

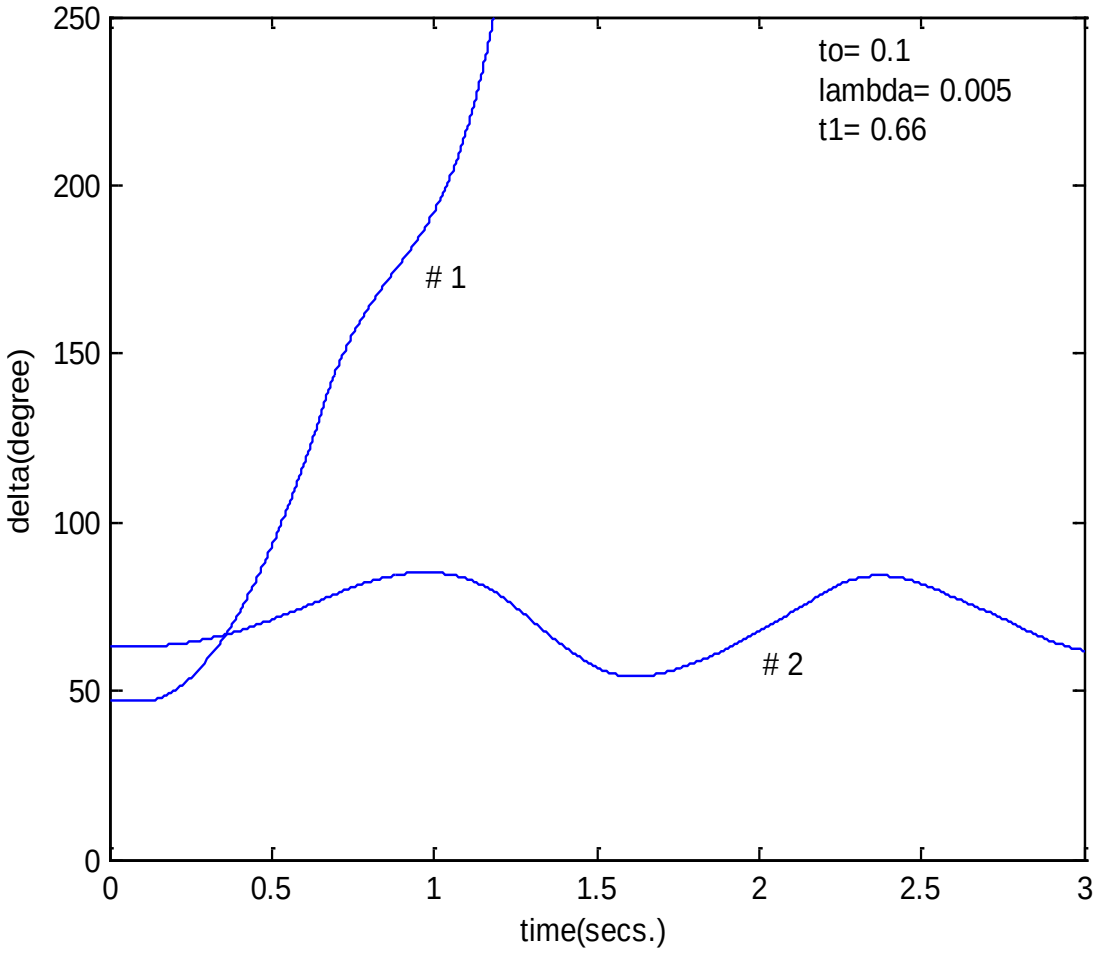

Fig.4.2(b): Power angle response without excitation control

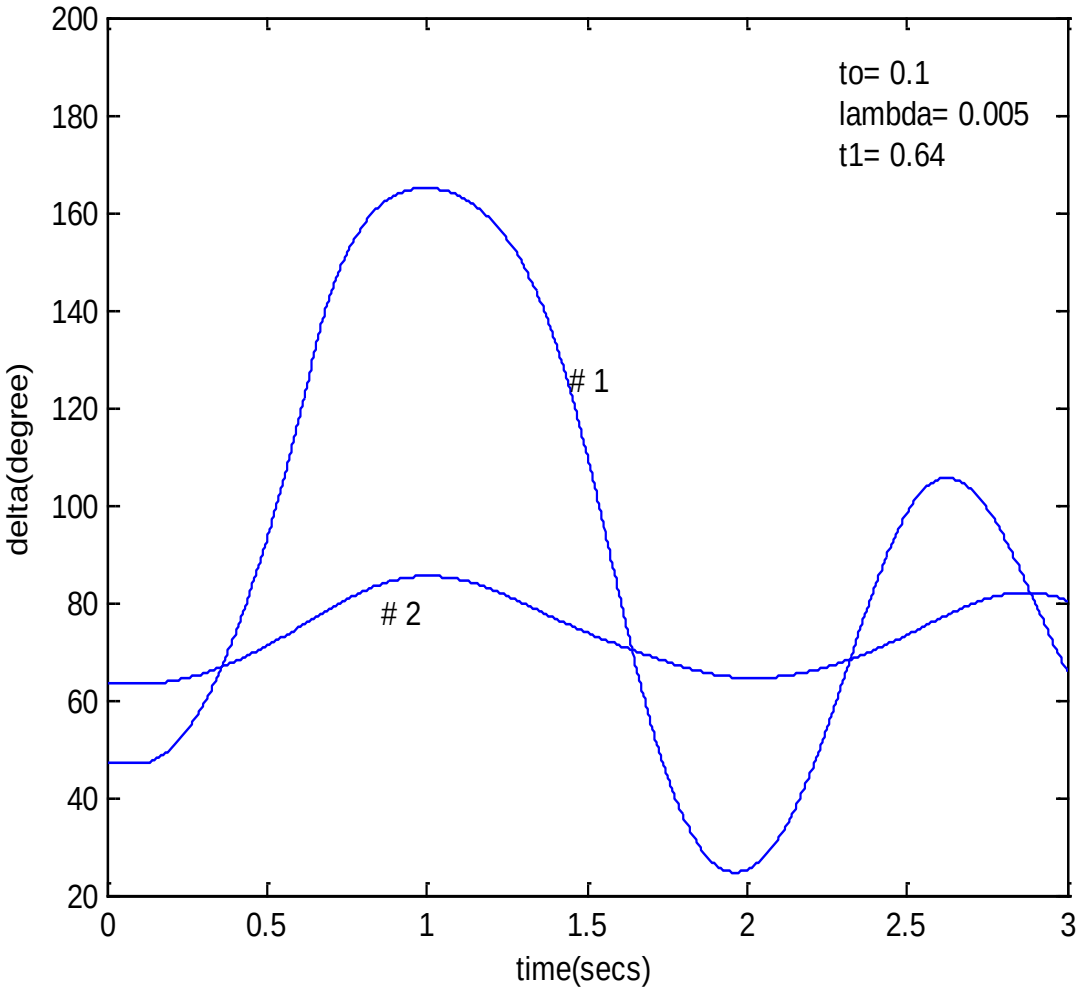

Fig.4.2(c): Power angle response with proposed excitation

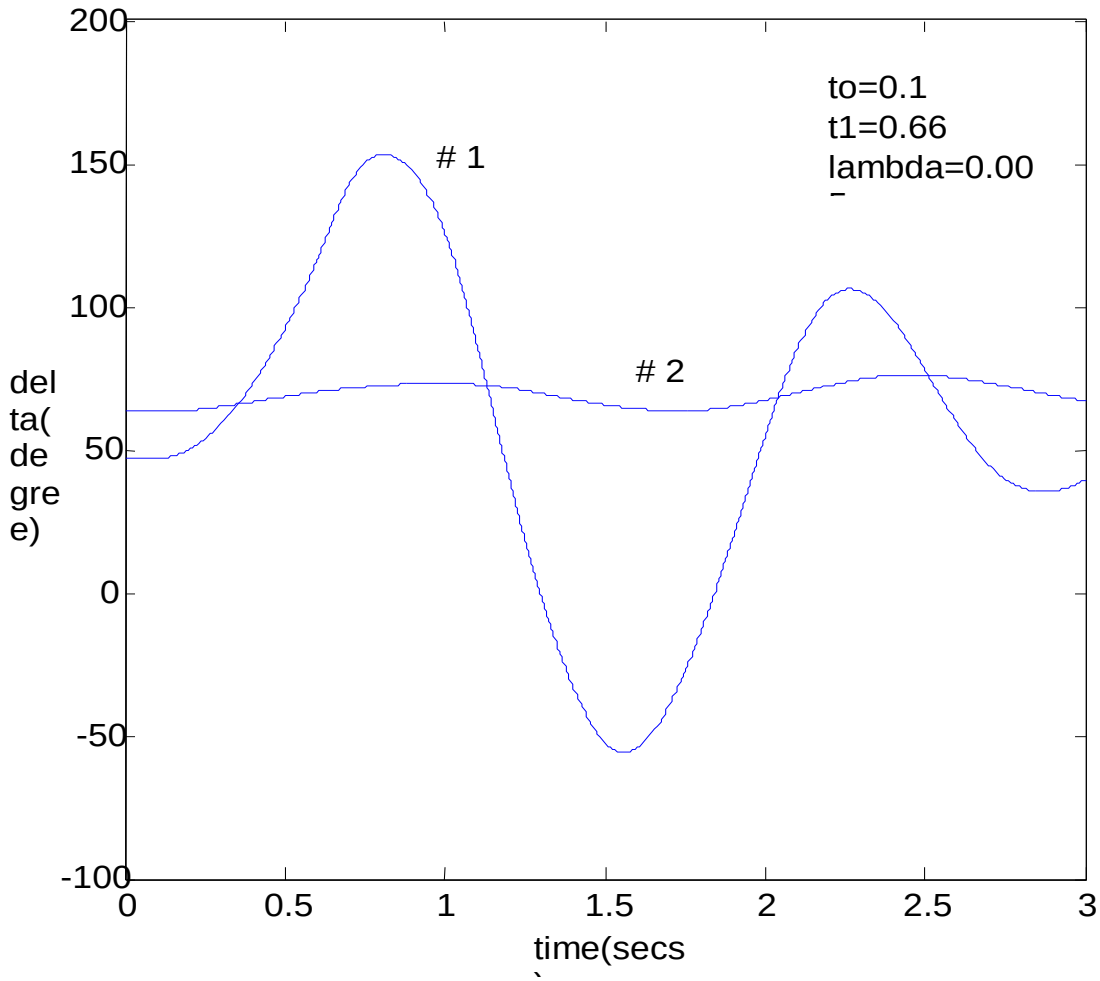

Fig.4.2(d): Power angle response without excitation control

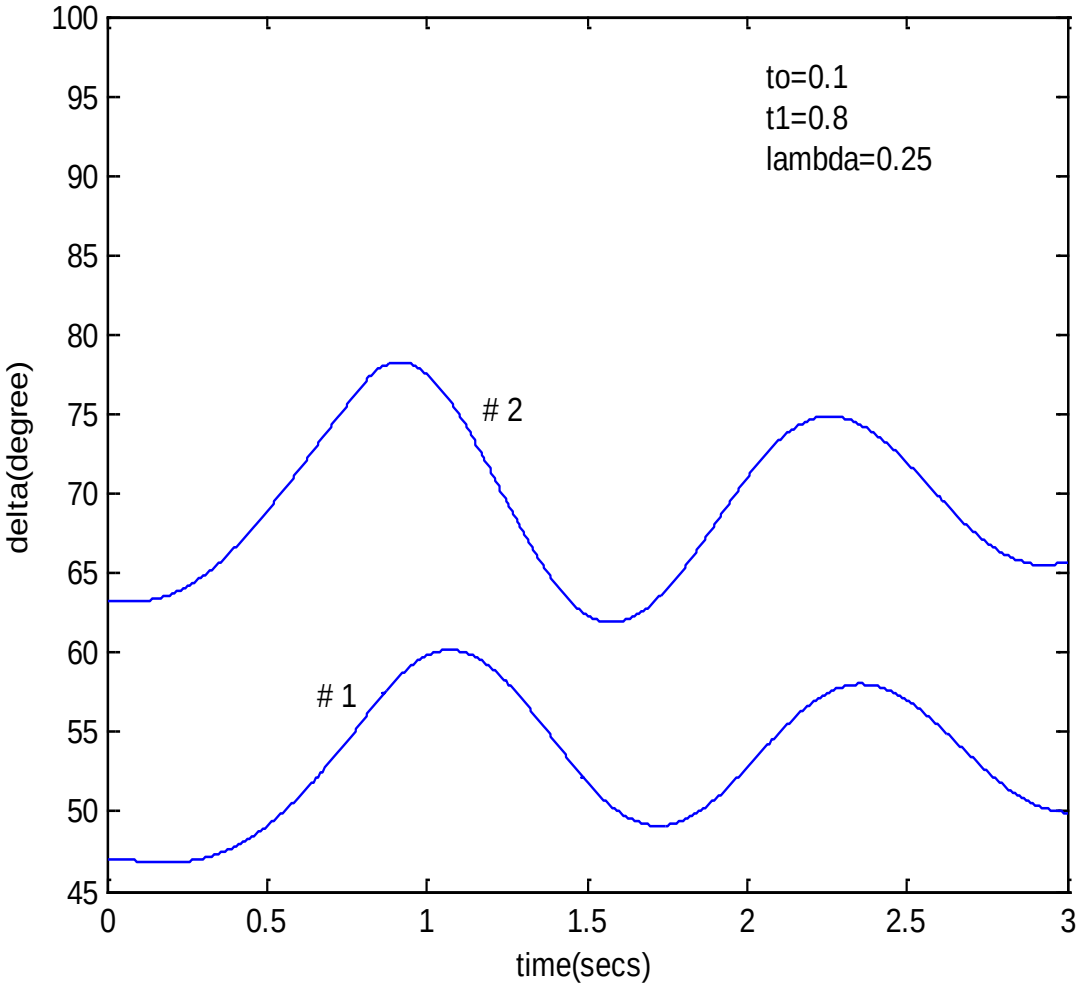

Fig.4.2(e): Power angle response with proposed excitation control

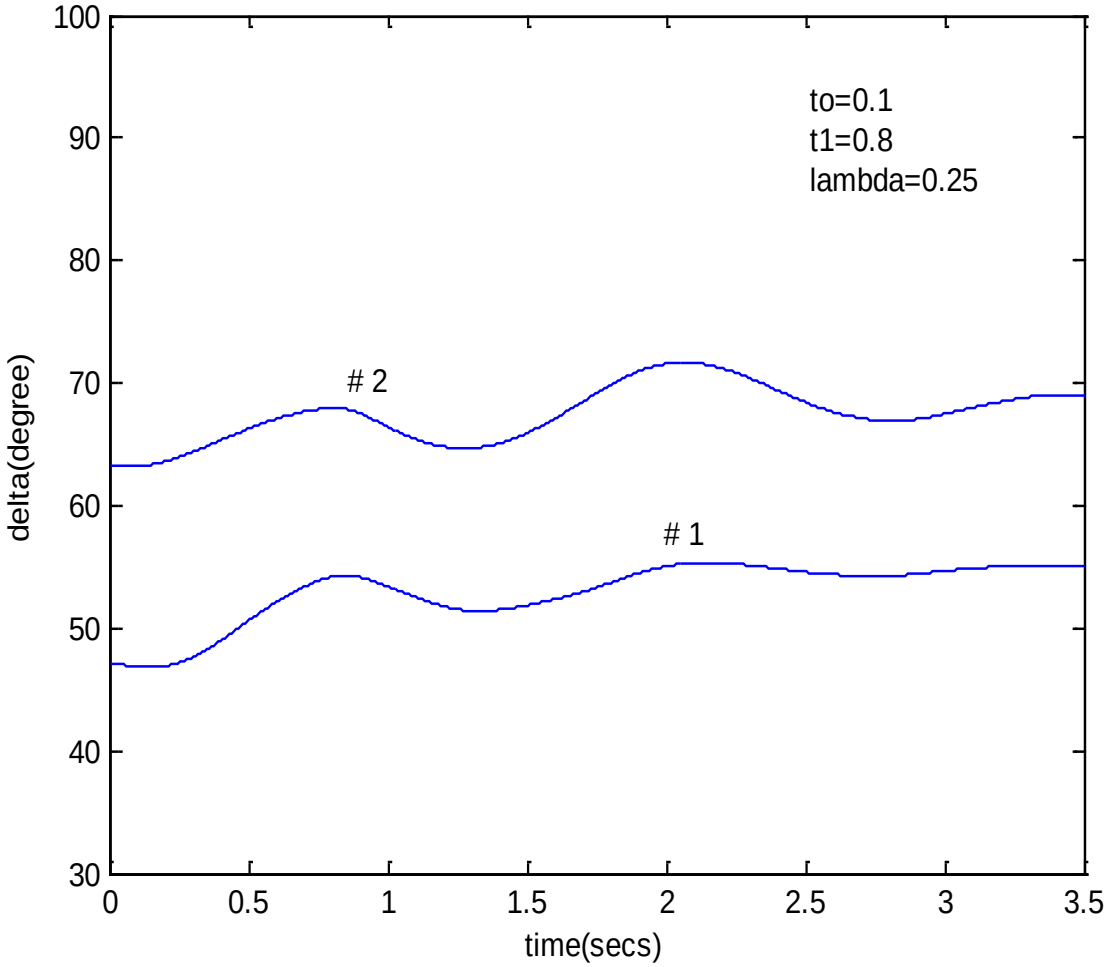

Fig.4.2(f): Power angle response without excitation control

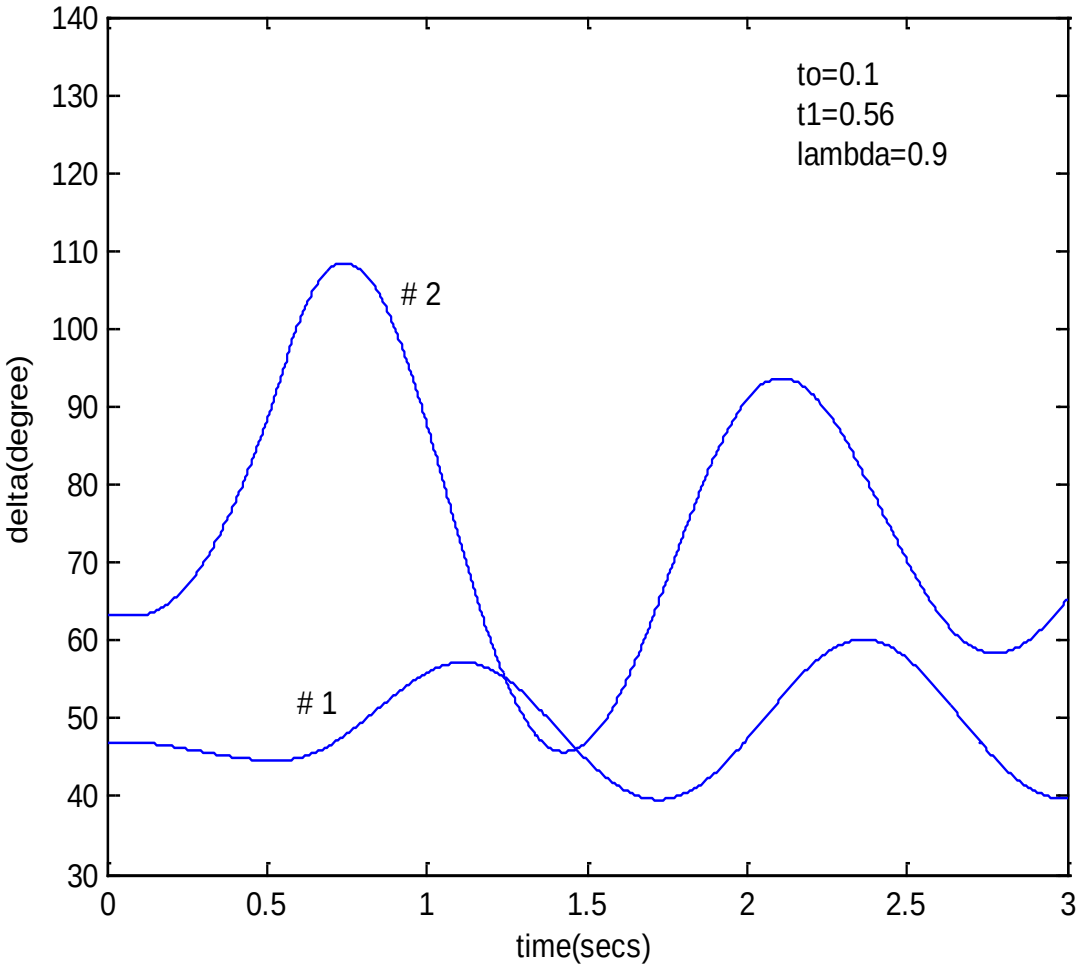

Fig.4.2(g): Power angle response with proposed excitation control

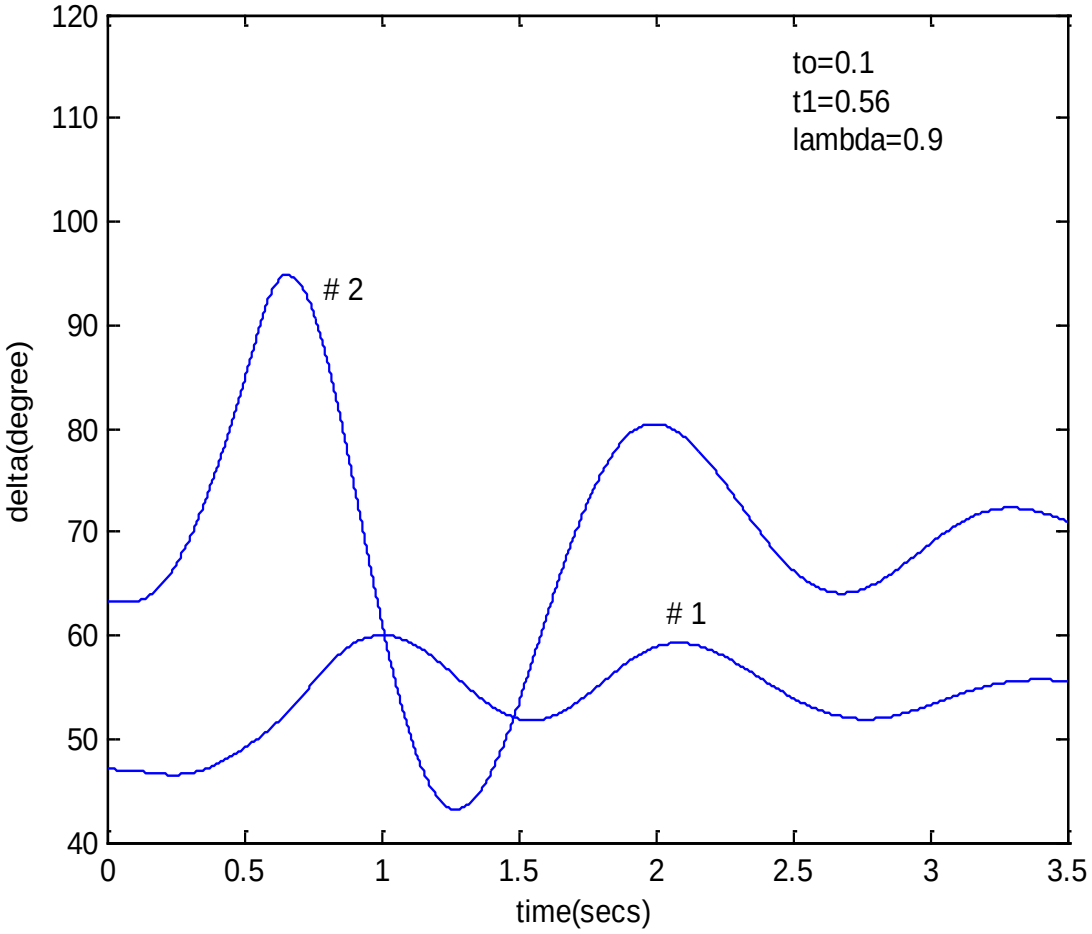

Fig.4.2(h): Power angle response without excitation control

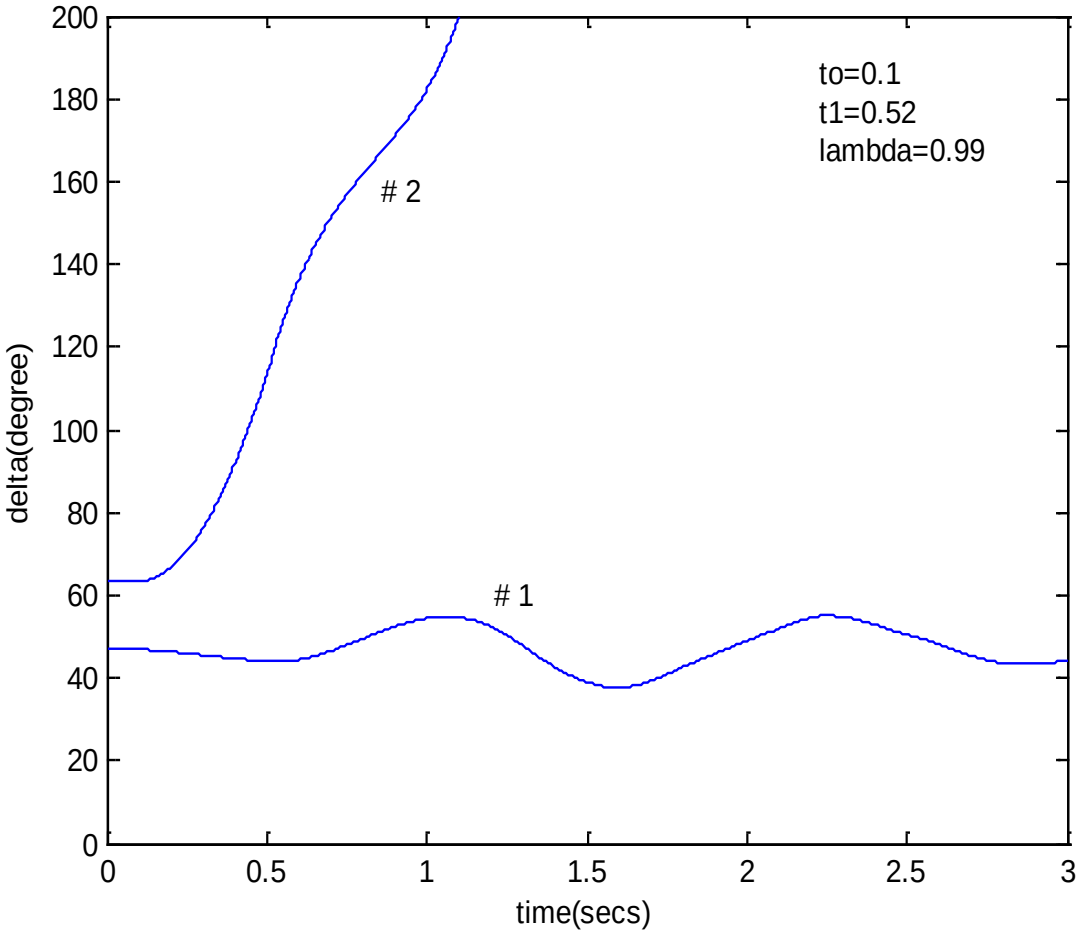

Fig.4.2(i): Power angle response without excitation control

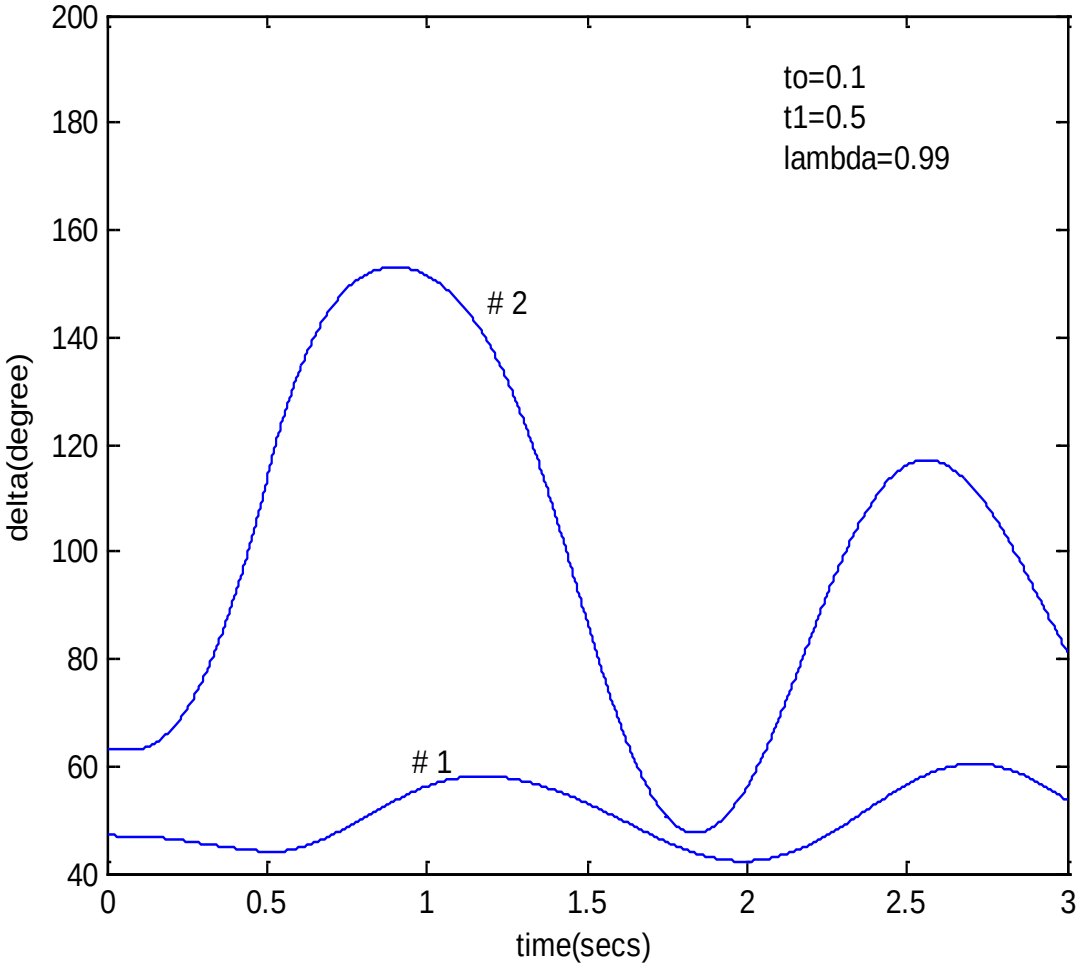

Fig.4.2(j): Power angle response with proposed excitation control

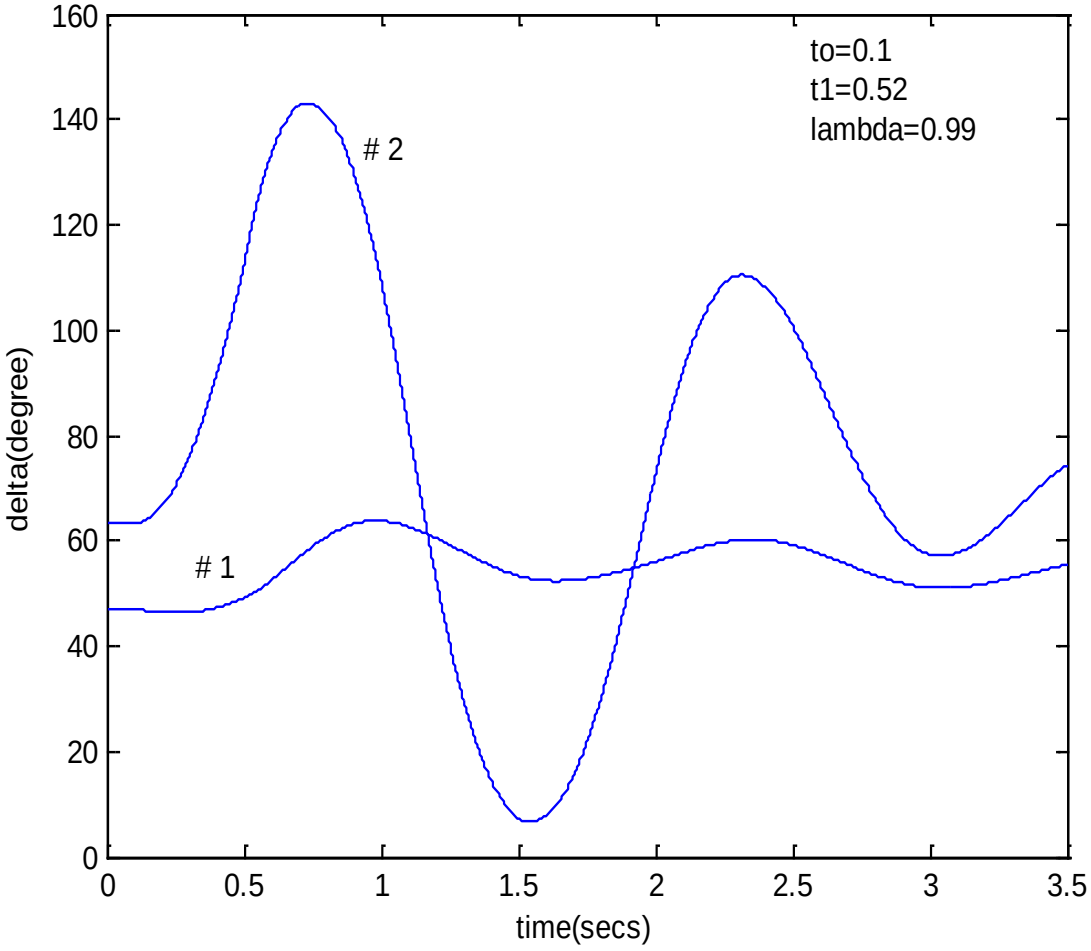

Fig.4.2(k):Power angle response with proposed excitation control

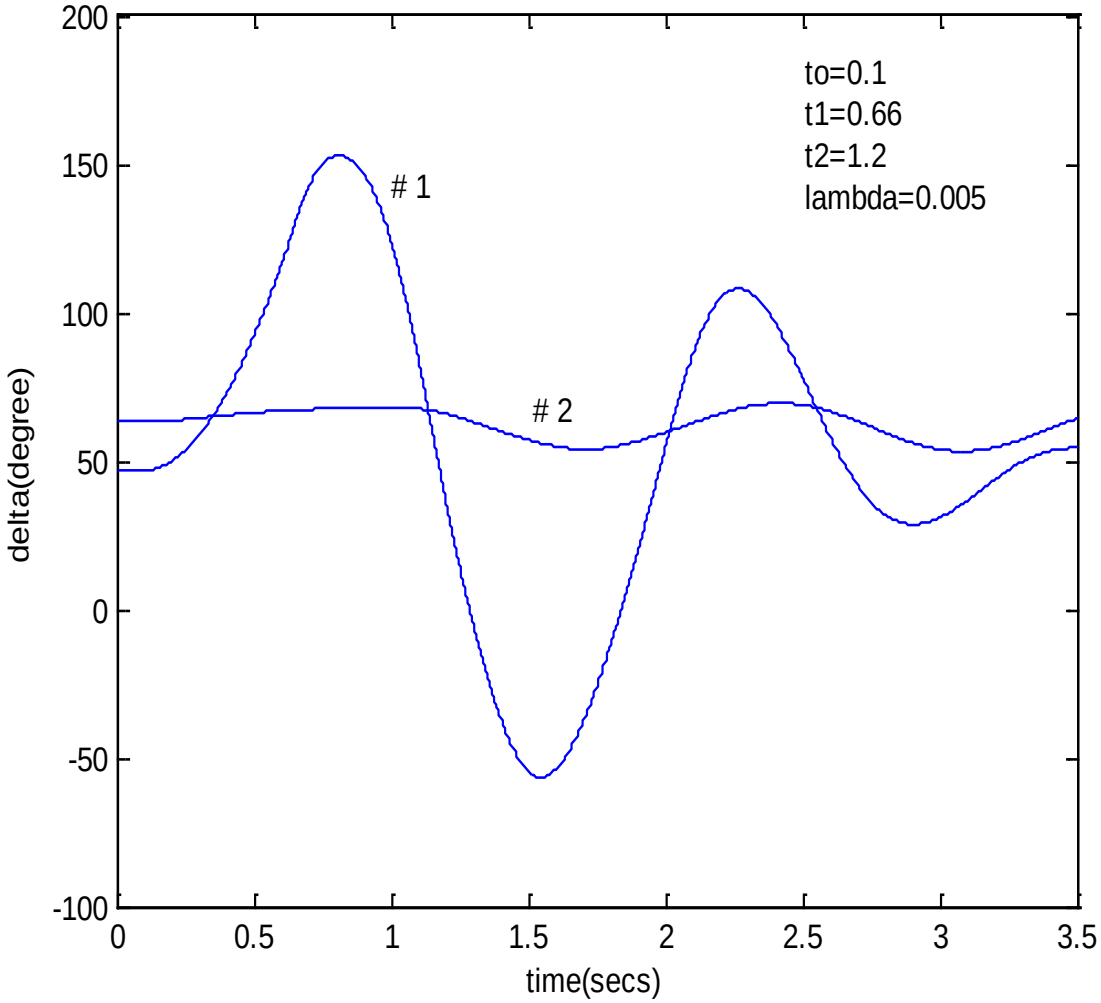

Fig.4.2(l): Power angle response with excitation control

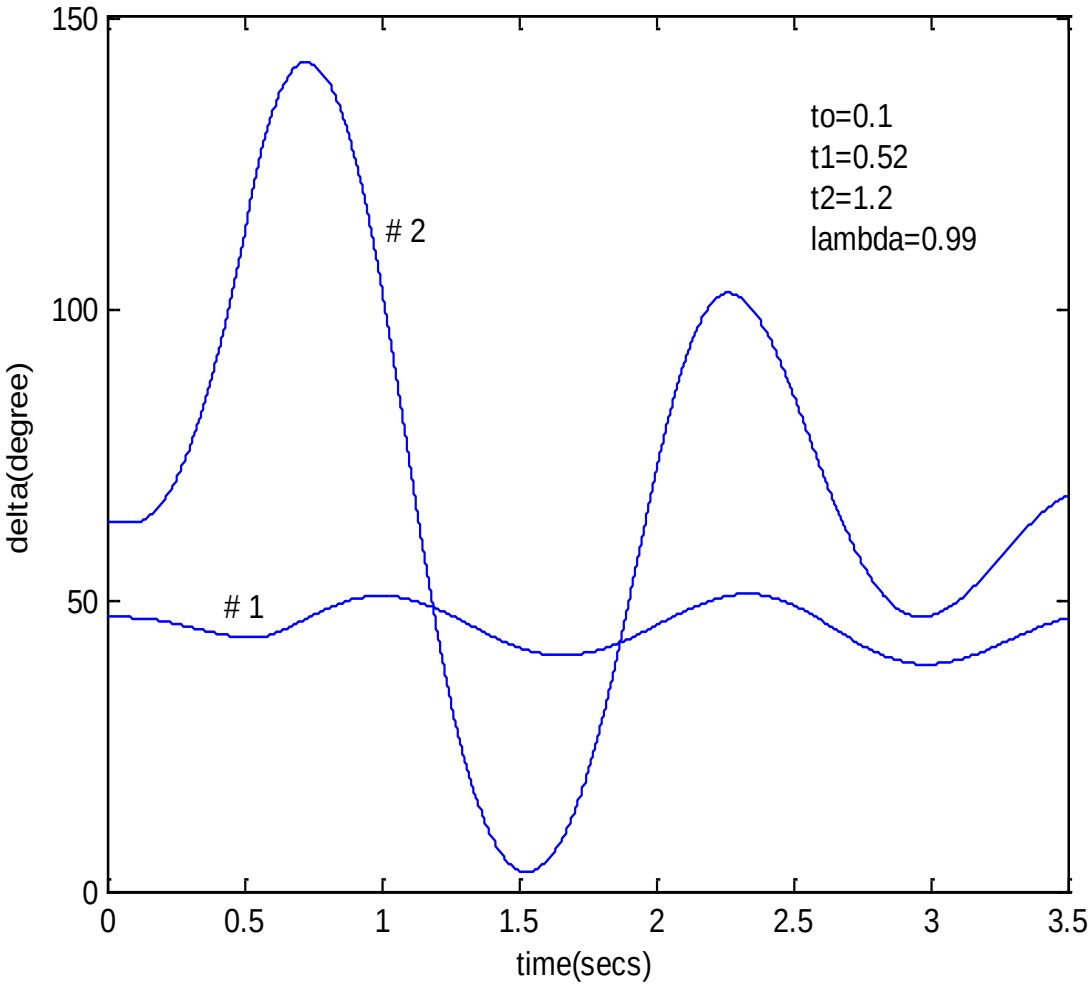

Fig.4.3(a): Power angle response

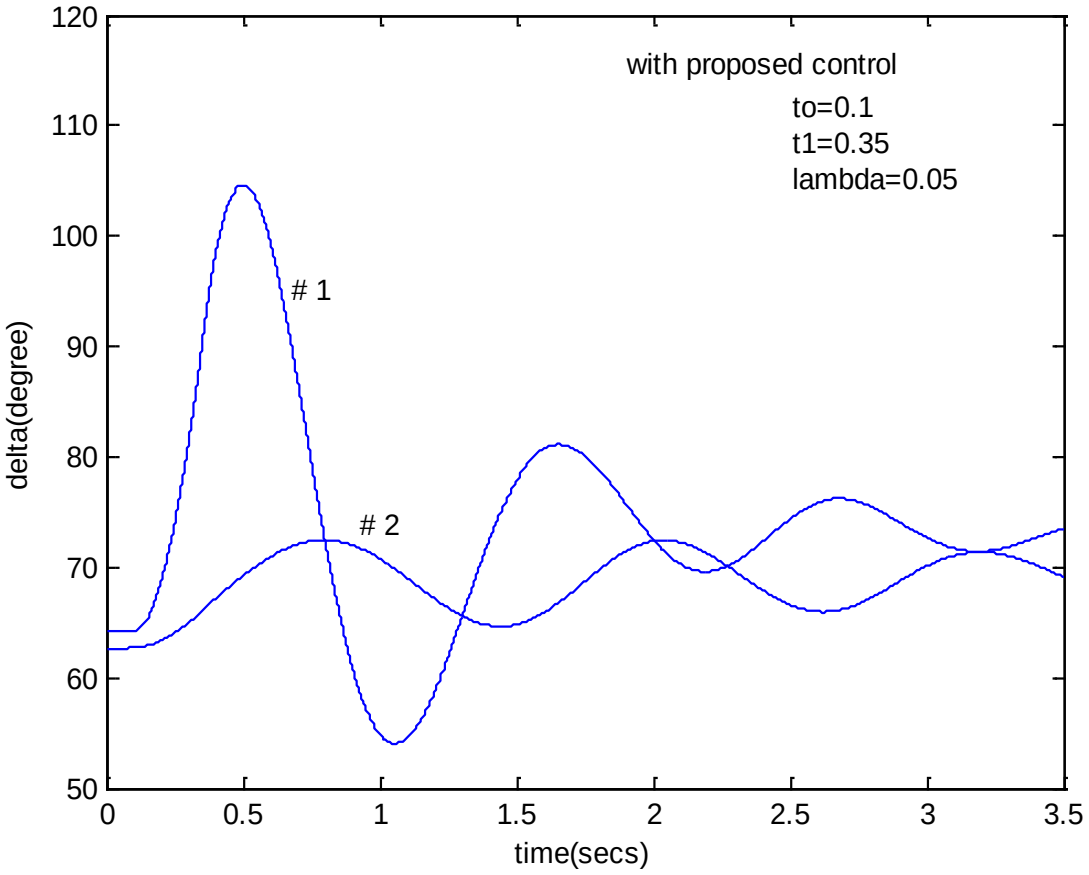

Fig.4.3(b): Power angle response

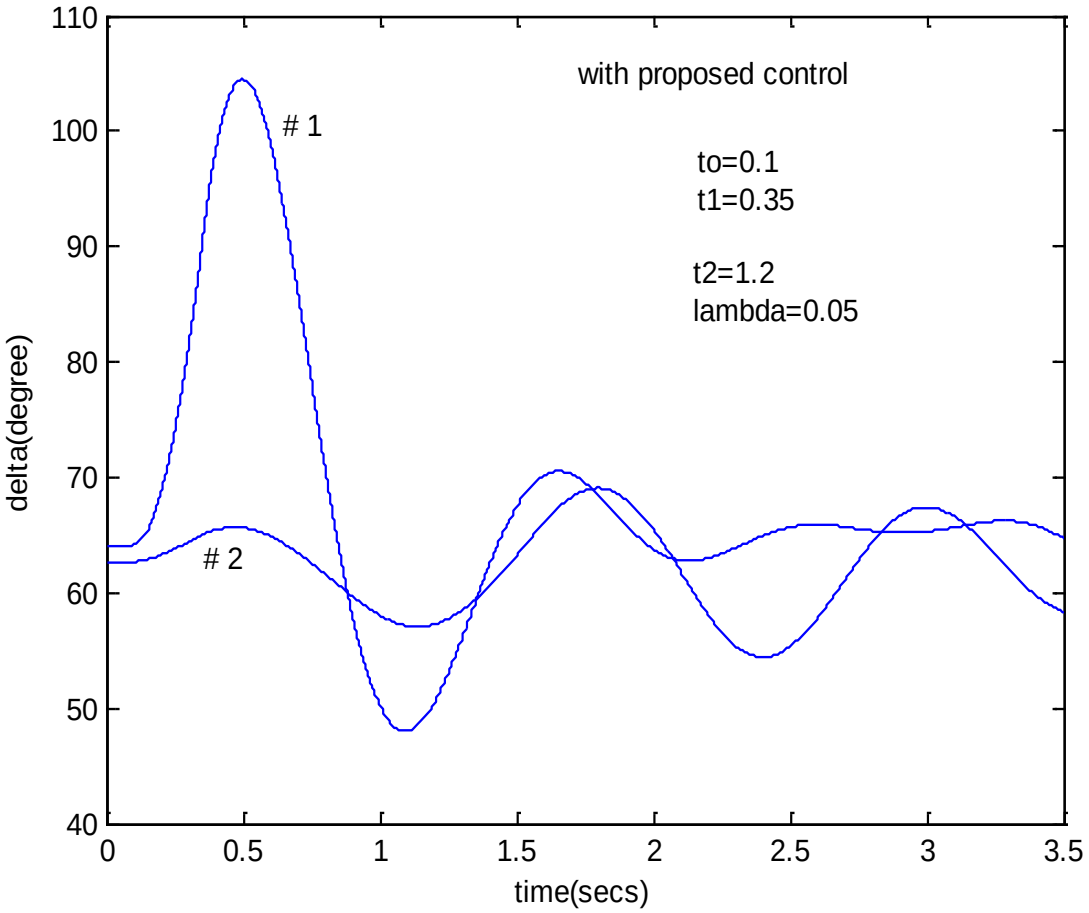

Fig.4.3(c): Power angle response

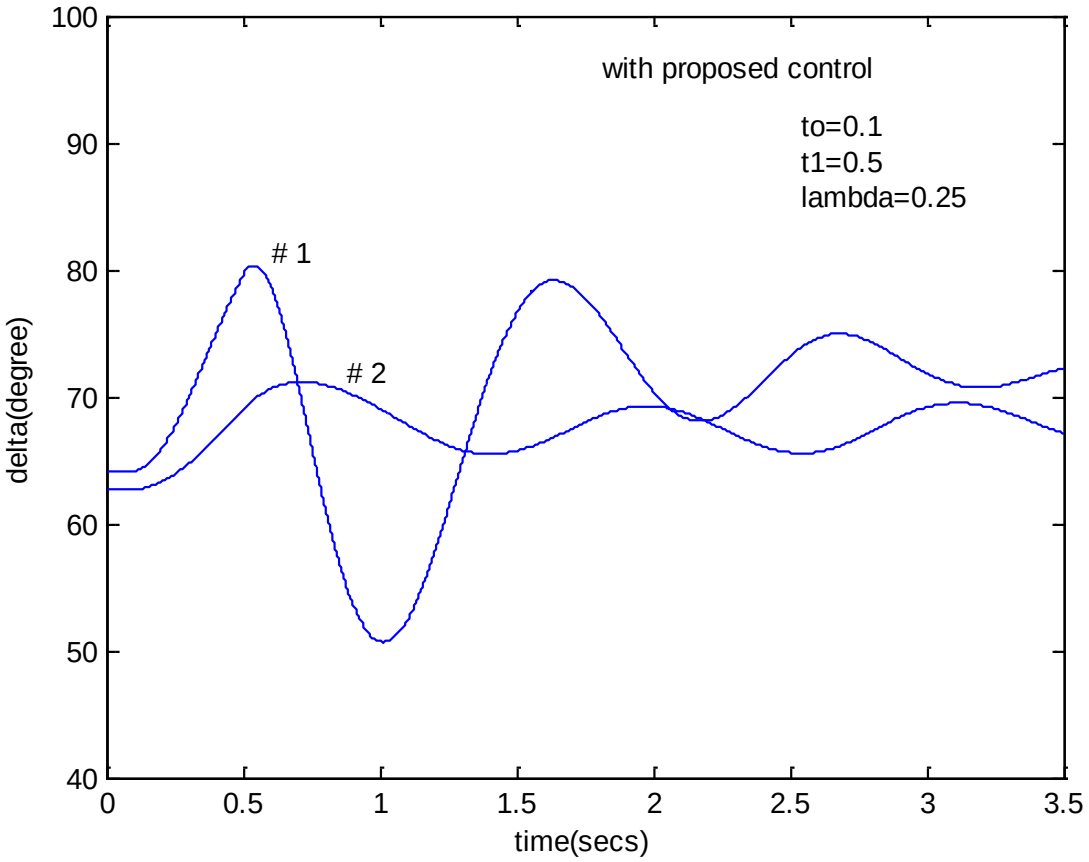

Fig.4.3(d): power angle response

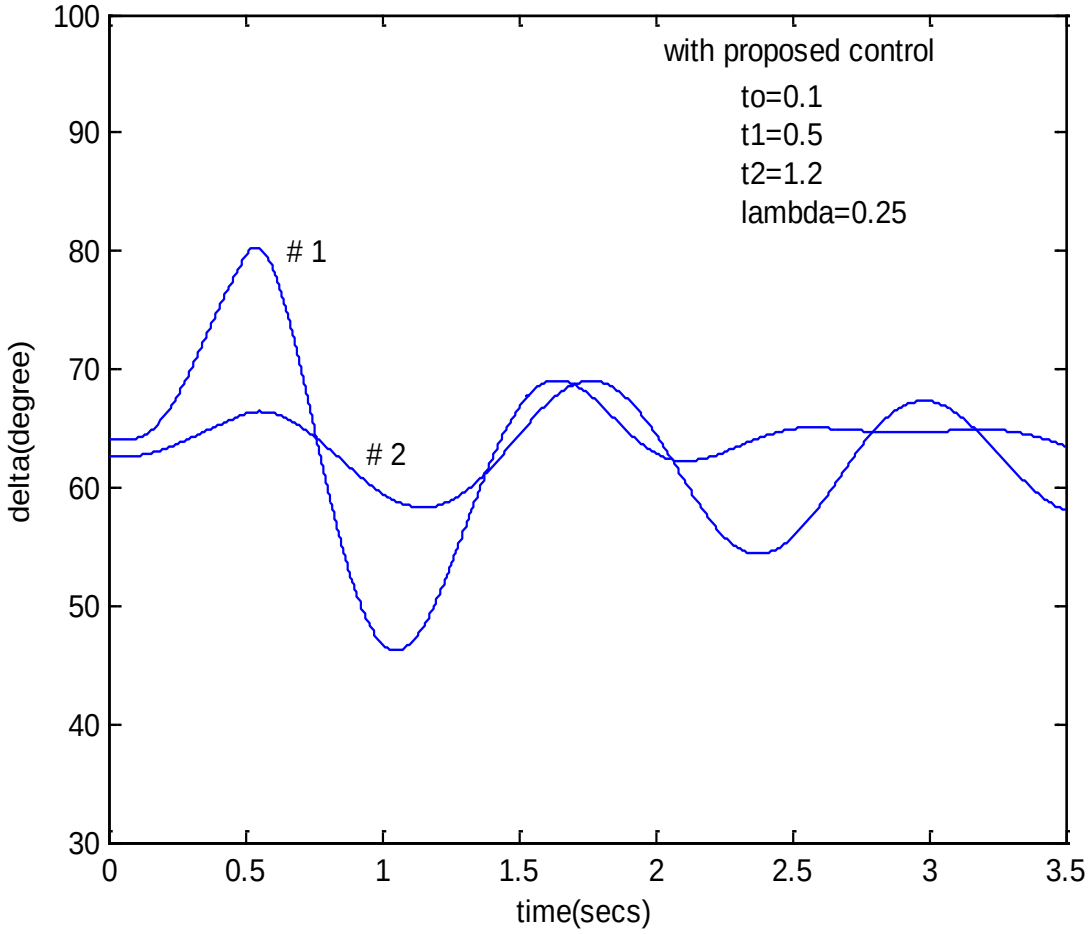

Fig.4.3(e): Power angle response

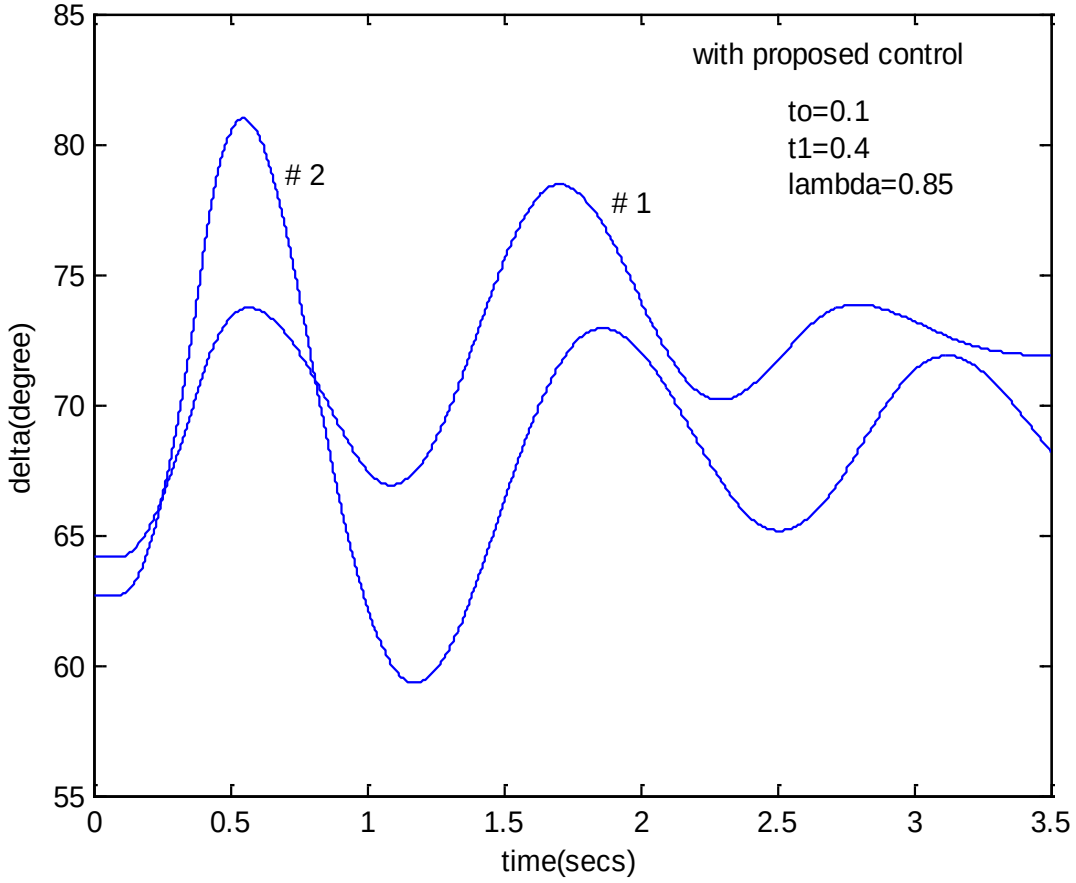

Fig.4.3(f): Power angle response